Inorganic Chemistry Communications 157 (2023) 111272

Contents lists available at ScienceDirect

Inorganic Chemistry Communications

journal homepage: www.elsevier.com/locate/inoche

Short communication

Cationic resin polymer A®IRC-50 as an effective adsorbent for the removal of Cr(III), Cu(II), and Ag(I) from aqueous solutions: A kinetic, mathematical, thermodynamic and modeling study

Jaouad Bensalah [a,*], Hanae Ouaddari [b], Şaban Erdoğan [c], Burak Tüzün [d], Abdel-Rhman Z Gaafar [e], Hiba-Allah Nafidi [f], Mohammed Bourhia [g], Amar Habsaoui [a]

[a] Laboratory of Advanced Materials and Process Engineering (LAMPE), Department of Chemistry, Faculty of Sciences, Ibn Tofaïl University, B.P. 133, 14000 Kenitra, Morocco
[b] Laboratory of Materials, Nanotechnology and Environment, Faculty of Sciences, Mohammed V University in Rabat, Av. Ibn Battouta, P.O. Box. 1014, Agdal-Rabat, Morocco
[c] Department of Nutrition and Dietetics, Faculty of Health Sciences, Yalova University, Yalova, Turkey
[d] Plant and Animal Production Department, Technical Sciences Vocational School of Sivas, Sivas Cumhuriyet University, Sivas, Turkey
[e] Department of Botany and Microbiology, College of Science, King Saud University, P.O. Box 11451, Riyadh, Saudi Arabia
[f] Department of Food Science, Faculty of Agricultural and Food Sciences, Laval University, 2325 Quebec City, QC G1V 0A6, Canada
[g] Department of Chemistry and Biochemistry, Faculty of Medicine and Pharmacy, Ibn Zohr University, Laayoune 70000, Morocco

ARTICLE INFO

Keywords:
Adsorption
Multivalent heavy metals
Cationic polymer A®IRC-50 resin
Adsorption Kinetics
Isotherm modelling

ABSTRACT

Adsorption has emerged as a reliable and cost-effective method for the depollution of wastewater containing multivalent heavy metals. However, there is still a need to optimize the process to achieve better efficacy. Consequently, This study focuses on the adsorption of three different metal ions, namely Cr (III), Cu (II), and Ag (I), using a cationic resin polymer called A®IRC-50 as the organic adsorbent. The high adsorption capacity of this polymeric material was investigated concerning various physicochemical parameters, including the dose of the cationic adsorbent, contact time, initial pH of the metallic solution, concentration of multivalent metals, and temperature (from 25 °C to 55 °C). The characterization of the adsorbent was performed using GTA/GTD, SEM spectroscopy, and EDX analysis. The kinetics of the adsorption phenomenally were evaluated exploited pseudo-1st-order and pseudo-2^{sec}-order models. The maximum amount of adsorption of the different metals studied are estimated at 171.33 mg.g^{-1} of the Cu(II), 90.16 mg.g^{-1} of the Cr(III) and 87.55 mg.g^{-1} of the Ag(I) at m = 0.1 g. The adsorption mechanism was determined by employing isothermal adsorption models such as Langmuir, Freundlich, and Temkin. The experimental results present demonstrated that the adsorption kinetics of the metals on the cationic polymer A®IRC-50 resin followed the pseudo-second-order model(100 mg.g^{-1} of Cr(III), 166.67 mg.g^{-1} of Cu(II) and 100 mg.g^{-1} of Ag(I)). The adsorption isotherms of the multivalent metal cations by the cationic polymeric A®IRC-50 resin were well-described by the Freundlich model, and the maximum capacities of the adsorption process were determined using the Freundlich isothermal model equation. The adsorption of multivalent heavy metals on the artificial polymer was found to be spontaneous and endothermic. The obtained ΔH values (46.85 Kj.mol^{-1}, 31.61 Kj.mol^{-1} and 35.50 Kj.mol^{-1} of the various metals Cr(III), Cu(II) and Ag(I) respectively), suggest that the interactions between the cationic polymer A®IRC-50 resin and the multivalent heavy metals are primarily physical. Finally, various thermodynamic technics between three metals study indicate as well ΔG° (−0.83 at −5.64 kJ. mol^{-1}) that the adsorption is impetuous and endothermic.

1. Introduction

The importance of water for the survival of living organisms is of utmost importance as it supports a variety of activities that are critical to life. The vitality of water is not only for human well-being but also serves as a source of natural resources that are essential for economic development. However, the scarcity of natural resources in water is becoming increasingly concerning and the state of the aquatic environment has

* Corresponding author.
E-mail address: Jaouad.bensalah@uit.ac.ma (J. Bensalah).

https://doi.org/10.1016/j.inoche.2023.111272
Received 21 June 2023; Received in revised form 13 August 2023; Accepted 19 August 2023
Available online 30 August 2023

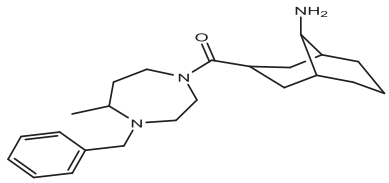

Fig. 1. The structure chemical of the organic polymer resin used in this study.

Table 1
A comprehensive overview of the modeling techniques utilized.

Kinetic Model	Equations	Parameters	Reference
Pseudo-1st Order	$\frac{dq_t}{dS} = K_1(q_e - q_t)$ (3)$\log(q_e - q_t) = \log(q_e) - \left(\frac{k_1}{2.203}\right).t$ (4)	q_t: Adsorption capacity at time present (mg/g) q_{eq}: Equilibrium capacity study (mg/g). k_1: The speed of 1st order (min^{-1}). t: The time study (min)	[10,11]
Pseudo-2^{sec} Order	$\frac{t}{q_t} = \frac{1}{k_2 q_e^2} + \frac{1}{q_e} \times t$ (5)	K_2: The constant of pseudo 2^{sec} order (g $mg^{-1}min^{-1}$)	[12–14]

Table 2
Equations utilized for the determination of the thermodynamic parameters studied.

Name of the equations	Equations	Parameters	Reference
Gibbs free energy	$\mathrm{Ln}(K_L) = \frac{\Delta S}{R} - \frac{\Delta H}{RT}$ (6) $\Delta G = \Delta H - T\Delta S$ (7)	$\Delta G°/\Delta H°/\Delta S°$: Energy Gibbs free/ Enthalpy / Entropy respectively (KJ.mol^{-1})/(kJ.mol^{-1})/(J.$mol^{-1}.K^{-1}$). T: Temperature (K)	[15]

deteriorated over time, mainly due to the discharge of untreated industrial waste into water bodies [1]. Notably, the discharge is often made up of toxic substances and chemical compounds studied, including various multivalent heavy metals, which have been confirmed to have detrimental effects on the aquatic environment and alter water quality. Among the various toxic substances, metals including chromium, copper, and silver are considered particularly hazardous due to their toxicity to ecosystems and their potentially deleterious effects on human health[2,3]. Copper is widely used heavy metal and is found in excess in industrial wastewater. Long-term exposure of copper induces nose and eye irritation, respiratory problems, neurotoxicity, and liver and kidney failure[2]. Noteworthy, these multivalent metals are generally heat resistant and are not readily biodegradable, making them persistent and potentially harmful. Hence, the efficient disposal of wastewater containing heavy multivalent metals remains a challenge for industries and environmentalists due to the current unavailability of cost-effective and efficient treatment options [3,4].

To preserve human health and environmental safety, techniques aimed at reducing the impacts of heavy metals on the aquatic environment have been developed, and they include adsorption, chemical precipitation, ion exchange, as well as membrane separation [4–6]. Of all the previously mentioned techniques, adsorption is often well-

Table 3
The various models used in the adsorption process isotherm party in this study.

Model's	Linearized equations	Parameters	Reference
Langmuir Isotherm	$\frac{C_e}{Q_e} = \frac{C_e}{Q_m} + \frac{1}{(K_L.Q_m)}$ (8)	Q_e/ C_e/ Q_m: Amount adsorbed/ Concentration in equilibrium/ Capacity maximum adsorption, respectively, (mg.g^{-1})/ (mg.g^{-1})/ (mg.L^{-1})/ (mg.g^{-1}). K_L: Constant equilibrium (L.g^{-1}).	[16]
Freundlich Isotherm	$\mathrm{Log}(q_e) = \log(K_F) + \frac{1}{n}.\log(C_e)$ (9)	K_F: Adsorption capacity constant ((mg.g^{-1})(L.mg^{-1}) 1/n). 1/n: Adsorption Intensity Constant.	[16,17]
Temkin Isotherm	$q_t = B_1 \ln(K_T) + B_1 \ln(C_e)$ (10)	b: Temkin constant (J.mol^{-1}) K_T: Temkin Isothermal Constant (L.g^{-1}) T: Temperature (K)	[17–19]

utilised due to its cost-effectiveness, versatility, and compatibility with existing water treatment systems [6,7]. Treatment of such wastewater to remove heavy metals and to make it consumable is a challenge for environmental researchers working in this field[7].

Notably, adsorption involves the adherence of substances majorly contaminant from gases or liquids onto the surface of a solid material, known as an adsorbent, and is commonly employed for the eliminate of organic and metallic contaminants from wastewater [8]. Adsorption is an effective, environmentally benign, attractive and alternative methodology for the extraction of toxic heavy metals from wastewater, adsorption has several priority aspects over other methods like easy availability of adsorbent, financially feasible treatment process, insensitivity of adsorbents to water pollutants and simple processing [7,8], have been reported for treatment of toxicmetal ions present in wastewater. Some of these methods have various disadvantages like high processing cost, sludge dumping formed as result of treatment, or unsuitability at large scale [9]. Adsorbents used during this process include activated carbon and activated alumina. Interestingly, the optimization of the adsorption process can be done by the utilization of a different adsorbent due to the crucial role they play in the selective capturing of target substances.

Herein, this study aims to explore cationic resin as the adsorbent for the adsorption of metals including Cr (III), Cu (II), and Ag (I) from wastewater, to study the kinetics of the absorption, to compare the predicted adsorption processes calculated with different models of excellent experimental behavior, in different advantages. Also, following the determination of the parameters that guide the adsorption using cationic resin, this study aims to optimize the adsorption pathways, investigate the dependence of adsorbent surface parameters on adsorption efficiency, determine adsorption capacities, and efficiently design adsorption systems based on the results obtained in this study.

2. Materials and methods

2.1. Reagents used and preparation steps

To investigate the pH, solutions of hydrochloric acid (HCl) and sodium hydroxide (NaOH) were utilized. Chromium (III) nitrate nonahydrate ($Cr(NO_3)_3(H_2O)_9$) (99.9%), copper (II) sulfate pentahydrate

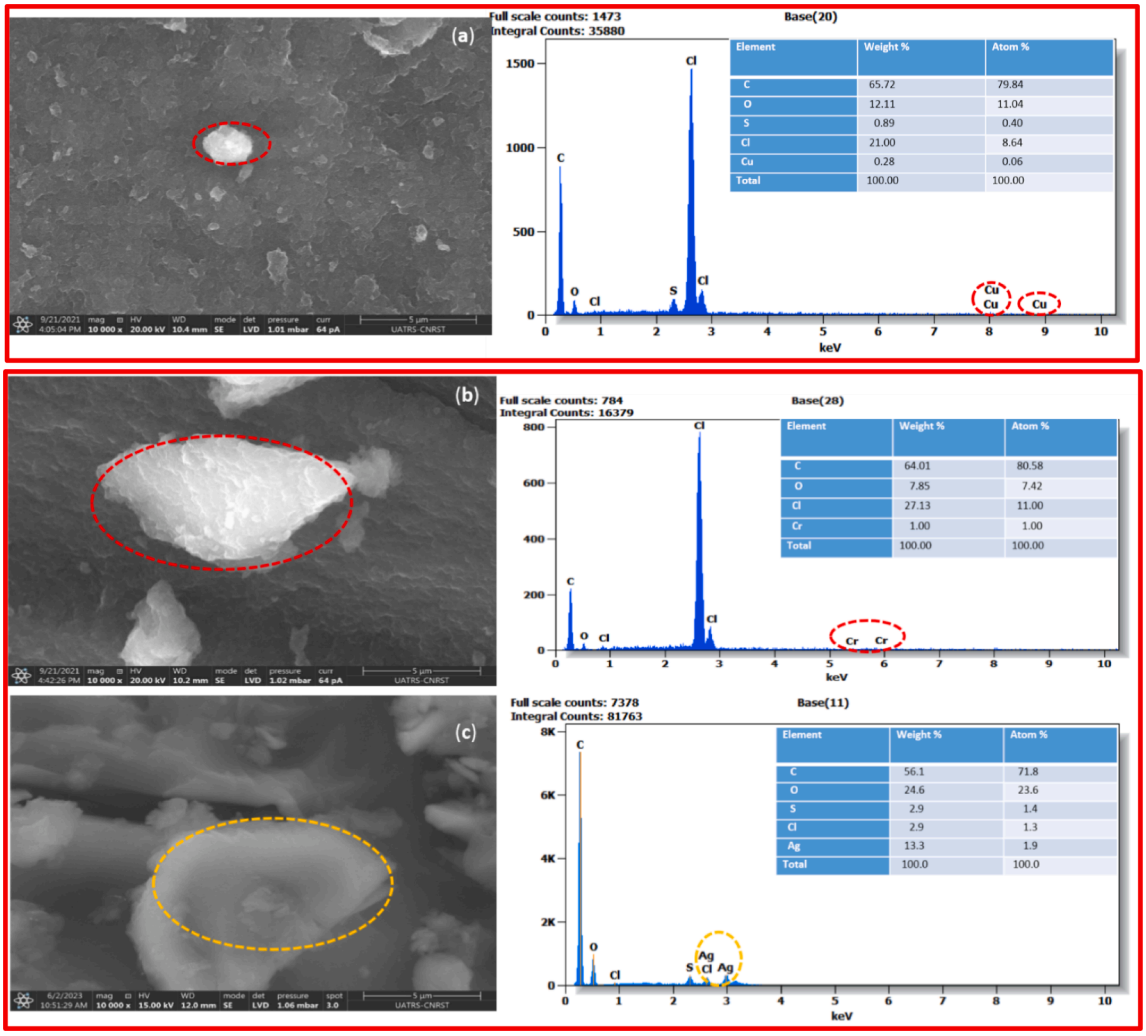

Fig. 2. SEM and EDX observation of the polymer resin organic without treatment and charged with Cu(II) **(a),** charged with Cr(III) **(b)** and charged with Ag(I) **(c).**

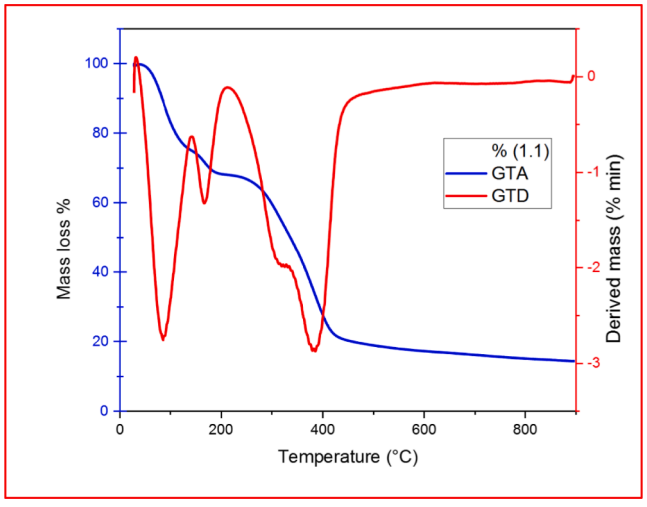

Fig. 3. TGA and GTD thermogram of the commercial adsorbent resin polymeric.

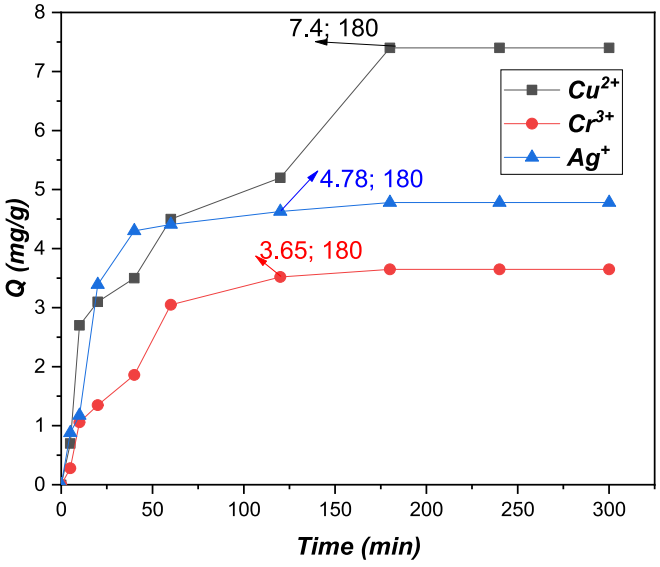

Fig. 4. The variation in the concentration of the various metals Cr (III), Cu (II) and Ag (I) ions as a function of contact time and pH for the A®IRC-50: $C_0 = 10$ mg.L^{-1}, V = 100 mL, T = 25° C and m = 0.1 g.

(Cu $(SO_4)(H_2O)_5$) (99%), and silver nitrate ($Ag(NO_3)$) (99%) were utilized as the source of the multivalent metal ions being studied. Noteworthy, the various solutions of the reagents were prepared using

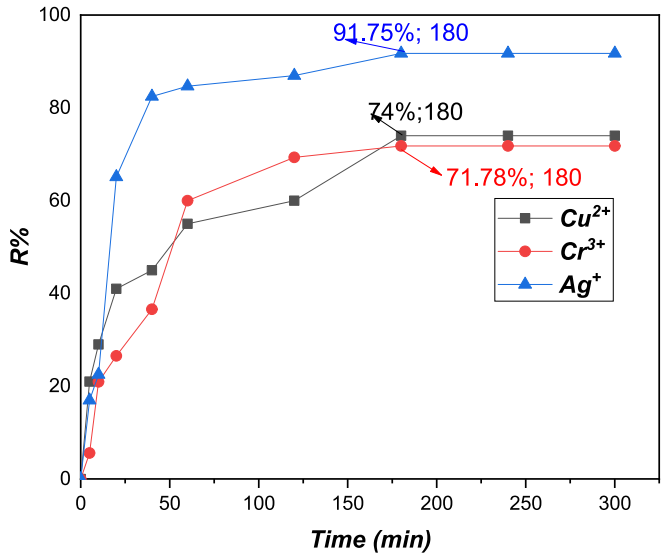

Fig. 5. The variation in the extraction yield of the various metals Cr (III), Cu (II) and Ag (I) ions as a function of the contact time present for the cationic resin A®IRC-50: C_0 = 10 mg.L^{-1}, T = 25° C, V = 100 mL, pH = 6.5 and m = 0.1 g.

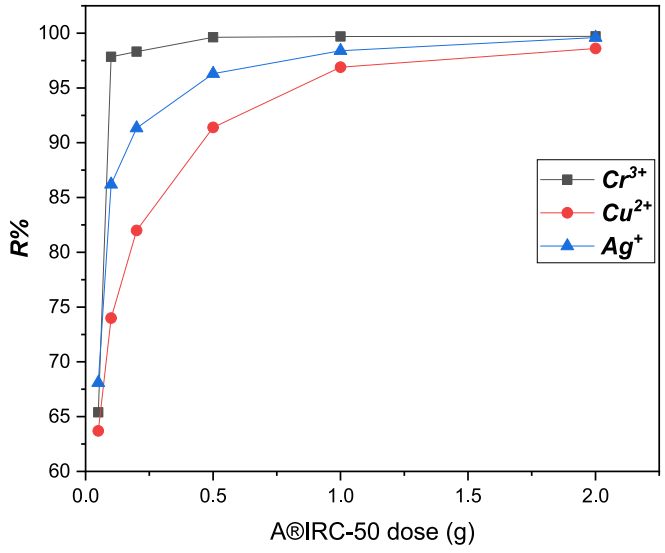

Fig. 6. Variation of the three different metals Cr (III), Cu (II) and Ag (I) Adsorption process as a function of time at various masses with [C] = 10 mg.L^{-1}, T = 25 °C and V = 100 mL.

distilled water.

2.2. The cationic organic polymer resin

The adsorbent polymer used in this study is cationic organic polymer resin with the chemical formula $C_{23}H_{37}Cl_2N_3O$ and the structure is depicted in Fig. 1.

In this study, the solid granules of the organic resin were utilized in the form of solid beads following subjection to purification by treatment with 1.0 M HCl. Subsequently, the resulting adsorbent was rinsed with distilled water.

2.3. Adsorption party experiments

2.3.1. Kinetic study of the adsorption contact

In this higher study, the study mode approach was employed to investigate the adsorption behavior of the polymer adsorbent which is the A®IRC-50 organic resin. Specifically, 0.1 g of the organic resin was brought in contact with a 100 mL solution containing different multivalent metal ions of interest in this study. Noteworthy, the pH of the solution was adjusted to accommodate the varying cationic multivalent metal ions. Subsequently, the A®IRC-50 organic resin was placed in a beaker along with the metal ions and stirred at a temperature of 298 K. Initially, the concentrations of the multivalent metals (Cr (III), Cu (II), and Ag (I)) were set at 10 mg/L for the study. Throughout the study duration, 1 mL of the different metallic solutions was withdrawn and transferred to 10 mL vials containing water. Hence, resulting in the automatic dilution of the high concentrations of the multivalent metal ions present in the solution. It is worth noting that befor each withdrawal, the mixture was stirred, ensuring that the total withdrawn volume did not exceed 10% of the initial volume of the respective metal ions' solution (Cr (III), Ag (I), and Cu (II)).

The concentrations of the multivalent metals (Cr (III), Ag (I), and Cu (II)) were measured using the AA240FS (AAS) and (ICP) spectrophotometry techniques. To calculate the adsorbed quantity (q) of each multivalent metal (Cr (III), Ag (I), and Cu (II)) at a given time (t), the adsorption capacity was determined by comparing the initial and instantaneous concentrations (C_0 and C_t) of the respective metal ions. This calculation was performed using Equations (1) and (2), respectively:

$$Q_e = (C_0 - C_e) \times \frac{V}{m} \quad (1)$$

$$R(\%) = \frac{(C_0 - C_e)}{C_0} \times 100 \quad (2)$$

Where:
C_o/ C_e: initial concentration/concentration at equilibrium (mg/L).
m: The mass of cationic polymeric (g).
V: The volume of multivalent ion solution (mL).

2.4. Different diffusion kinetic models of adsorption

To extensively understand the adsorption phenomena of the heavy multivalent metals being studied on the A®IRC-50 organic polymeric resin, this study employed thorough experimental techniques which were capable of ensuring saturation and widespread applicability. Table 1 presents the various models employed in this study.

2.5. Investigation of the thermodynamics parameters of the adsorption process

Studying the thermodynamic aspects of the adsorption process for different heavy metal ions in solution provides valuable insights into the underlying mechanisms involved in their adsorption. Notably, the investigation of thermodynamic parameters such as Gibbs free energy (ΔG°), enthalpy (ΔH°), and entropy (ΔS°), is capable of revealing significant information about the energetics and spontaneity of the adsorption process.

The determination of the values of (ΔH°, ΔS°), along with the slope and intercept of the aligned plot between the constant Ln (K) and 1/T, are crucial to understanding the thermodynamic behaviour of the adsorption process. Table 2 presents the equation utilized for the determination of the value of the ΔG °.

2.6. Adsorption party of the isotherm kinetic

To study the adsorption isotherms, the initial concentrations of the

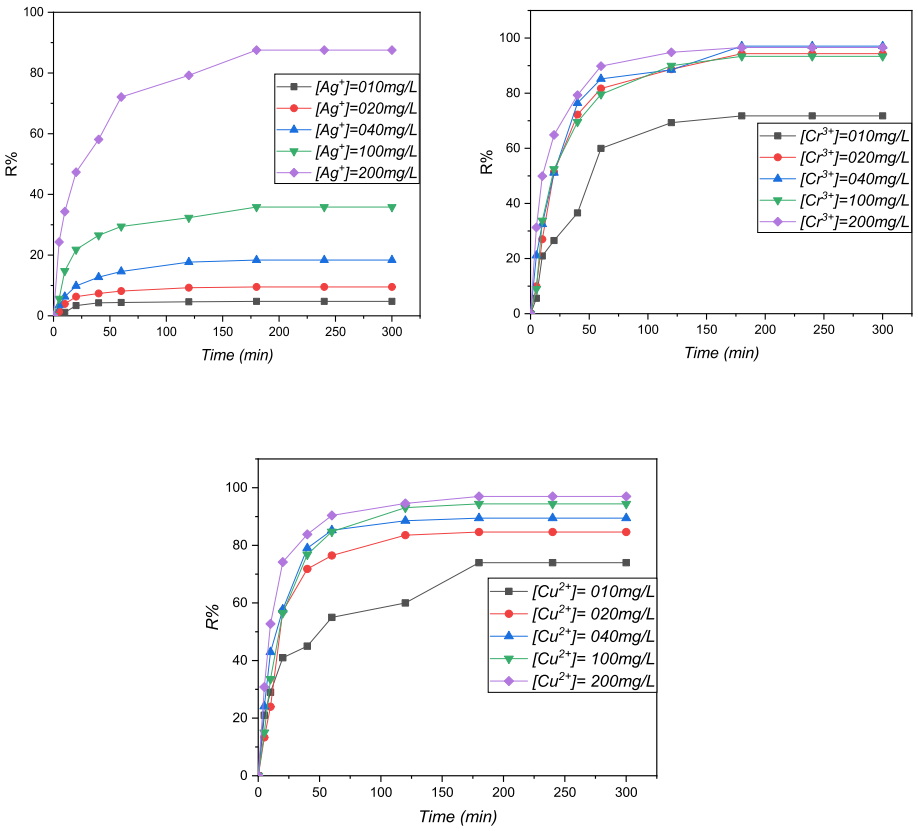

Fig. 7. The variation in the binding capacity of the adsorbent for the three different metals Cr (III), Cu (II) and Ag (I) ions, as a function of the contact time at the different concentrations for the cationic resin A®IRC-50: T = 25° C, V = 100 mL, m = 0.1 g.

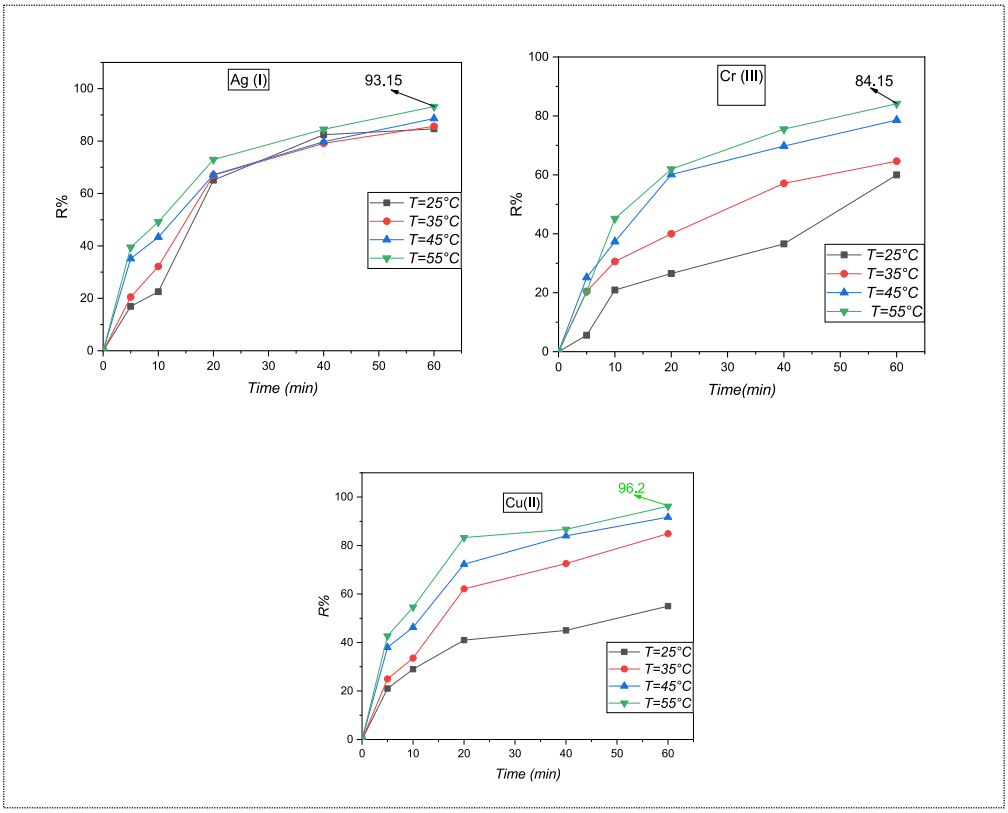

Fig. 8. The variation in the extraction yield of the different metals cr (iii), cu (ii) and ag (i) ions as a function of the temperature of the resin a®irc-50: $c_0 = 10$ mg.L^{-1}, V = 100 mL, pH = 6.5, m = 0.1 g, t = 60 min.

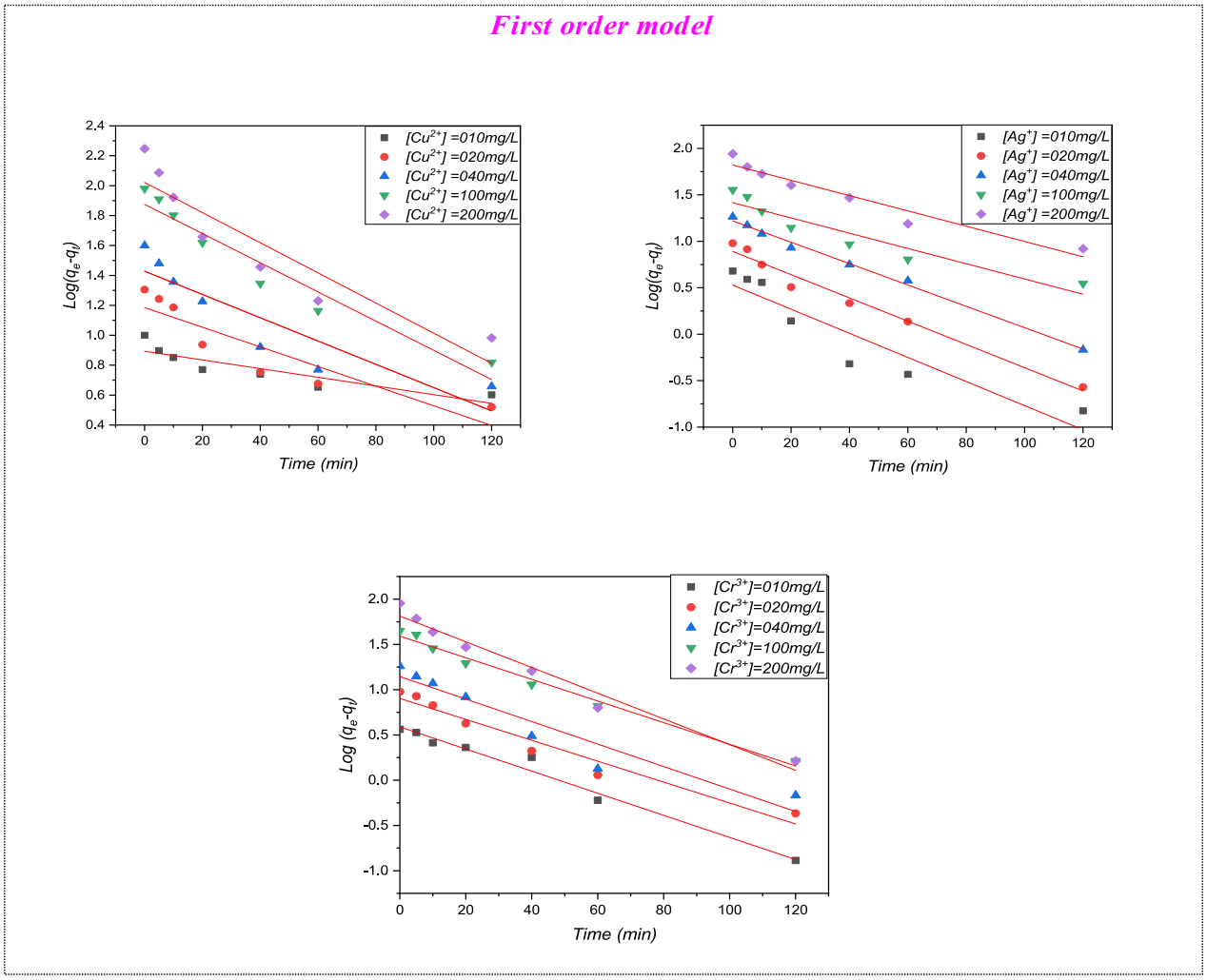

Fig. 9. Pseudo-first order kinetic model of the different metals Cr (III), Cu (II) and Ag (I) ions.

various multivalent cationic metals being studied were altered. Notably, the concentration ranged from approximately 10 mg.L^{-1} to 200 mg.L^{-1}, while a fixed adsorption contact time determined in the kinetics process test study was maintained. Ultimately, the samples were taken and subjected to analysis using ICP and AAS, upon reaching the point of saturated contact time. It is worth noting that the adsorption isotherm study examines the relationship between the different metal ions present in the solution and those adsorbed by the cationic resin when they are in equilibrium. This study provides valuable information about the parameters involved in designing adsorption systems, as well as the nature and mechanisms involved in the process. The isotherm models studied in this research were Langmuir, Freundlich, and Temkin, the results are presented in Table 3.

2.7. Molecular dynamic calculations

Monte Carlo simulations have emerged as a powerful computational tool extensively utilized to investigate potential adsorption-metal interactions in numerous adsorption systems. Hence, in this study, the Materials Studio 6.0 software was employed to conduct these calculations using the Condensed-phase Optimized Molecular Potentials for Atomistic Simulation Studies (COMPASSII) force field. The selected metals for interaction with the corrosion inhibitor were Cr, Ag, and Cu, which are being studied. The energy of the simulation system after the removal of water molecules is termed the total energy (E_{tol}), while the $E_{surface}$ and E_{inh} are the energy of the metal surface and the energy of the inhibitor molecules respectively [20].

3. Results and discussion

3.1. Characterization

3.1.1. Scanning Electron Microscopy (SEM) / energy-dispersive X-ray (EDX) spectroscopy analyses

The Scanning Electron Microscopy (SEM)-derived images which depict the characteristics of the crude cationic polymer organic A®IRC-50 resin are presented in Fig. 2. Following a thorough observation of Fig. 2 which depicts the resin in its original state, it is evident that the resin's surface morphology exhibits a porous structure. Notably, this porous and irregular reinforcement confirms its suitability as an adsorbent material. Conversely, a thorough observation of Fig. 2 which depicts the resin after subjection to a washing process using hydrochloric acid (HCl), reveals the presence of strong white surfaces, which can be attributed to the adsorption process facilitated by the addition of HCl, the exploited results have already been published in a previous work [22]. Furthermore, these surfaces are attributable to the binding of various cationic multivalent ions such as Ag(I), Cu(II), and Cr(III).

The obtained energy-dispersive X-ray spectroscopy (EDX) diagram, as depicted in Fig. 2, displays the presence of the metal copper (Cu) peaks in the adsorbent spent A®IRC-50 material. However, upon subjecting the support to a washing process with hydrochloric acid (HCl), it becomes evident that the traces of copper originally present in the

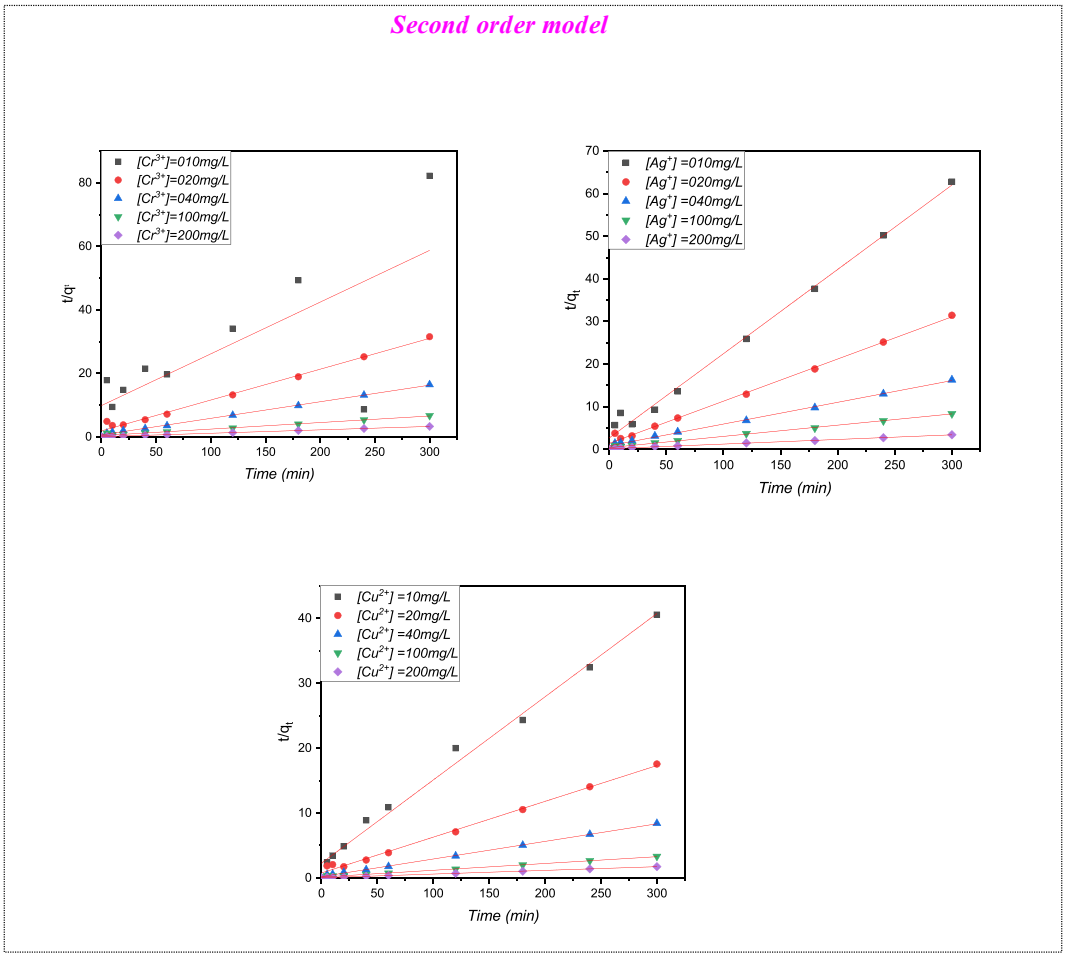

Fig. 10. Pseudo-second order kinetic model of the different metals Cr (III), Cu (II) and Ag (I) ions on the resin A®IRC-50 beads.

material are effectively eliminated, as depicted in Fig. 2.

3.1.2. The analysis of the thermostability of the adsorbent (TGA)

The thermal stability analysis of the cationic organic adsorbent polymeric resin and the filter adsorbed with various multivalent metal ions was conducted using gravimetric analysis. The study involved subjecting the samples to a temperature ramp of −1°C/min. The resulting mass change percentages were obtained and their derivative with respect to temperature, which spanned from 293 K to 1073 K was determined and the results are depicted in Fig. 3. The temperature range studied spanned from 293 K to 1073 K, and the results are illustrated in Fig. 3.

The initial mass loss observed in the cationic adsorbent polymeric resin occurred at approximately 373 K, and this can be attributed to the evaporation of water. The water content in the resin is estimated to be around 20%, which may vary depending on the relative humidity of the ambient air. Similarly, a notable event is observed in the temperature range of 80–360 °C, indicating the thermal degradation of the cationic adsorbent polymeric resin. Notably, the peak derived at 80 °C and a narrow shape 360 °C, signifies the degradation of the pure resin material. The residues obtained at temperatures above 800 °C account for approximately 0.84% of the initial mass. Noteworthy, the thermal stability of pure materials, including the cationic adsorbent polymeric resin, can be influenced by factors such as surface morphology or sampling. Similar analyses were conducted using an extract derived from reed, with the water content estimated to be 5.5%. The maximum derivative peak is observed at 300.33 °C. Residues obtained at temperatures exceeding 850 °C represent approximately 1.8% of the initial mass.

3.1.3. Impact of the contact time study

The contact time is an important parameter that influences the efficacy of the adsorption process, hence, its impact on the efficacy of the adsorption process of the metals being studied herein was assessed and the results are depicted in Fig. 4. As evident in Fig. 4, the adsorption efficacy during the initial 20 min of contact with the different metals was quite volatile. However, it achieved stability after approximately 180 min for the various metal ions. Interestingly, these outcomes align with the results of previous studies on the adsorption process of diverse metal ions utilizing different resin types [20–22]. Also, Fig. 4 presents the simultaneous evolution of the pH values in the various cationic metal solutions and the adsorption capacity (Qe) as a function of time.

Similarly, the results depicted in Fig. 5 reveal that there is a high extraction yield of approximately 60% within the first 50 min for the various metals. This indicates a strong affinity between the cationic adsorbent polymer resin and the lead cations. Progressively, the extraction yield increases and reaches a near-equilibrium state after 120 min, with values of 71% for Cr (III), 74% for Cu (II), and 91.78% for Ag (I) ions.

Further analysis of the graph depicted in Fig. 5 reveals that the adsorption capacity is optimal at around 60 min for Cr (III), Cu (II), and Ag (I) ions. Notably, the adsorption process initially exhibits a rapid step followed by a slower adsorption rate. This kinetic study indicates that the adsorption sites on A®IRC-50 resin gradually become occupied by the various metal ions, namely Cr (III), Cu (II), and Ag (I) ions. As evident by the stability in the curves presented in Fig. 5, the saturation capacities achieved in this experimental setup are Q_{max} (Cu^{2+}) = 7.4 mg.g^{-1}, Q_{max} (Cr^{3+}) = 3.65 mg.g^{-1}, and Q_{max} (Ag^{+}) = 4.78 mg.g^{-1}. These results closely align with previous studies involving the adsorption of

The Freundlich isotherm model assumes a multilayer adsorption phynomenally process and considers the solid surface morphology of the adsorbent organic resin to be heterogeneous [41,42]. The Freundlich equation, in its linear form, is given by the equation shown in Table 4.

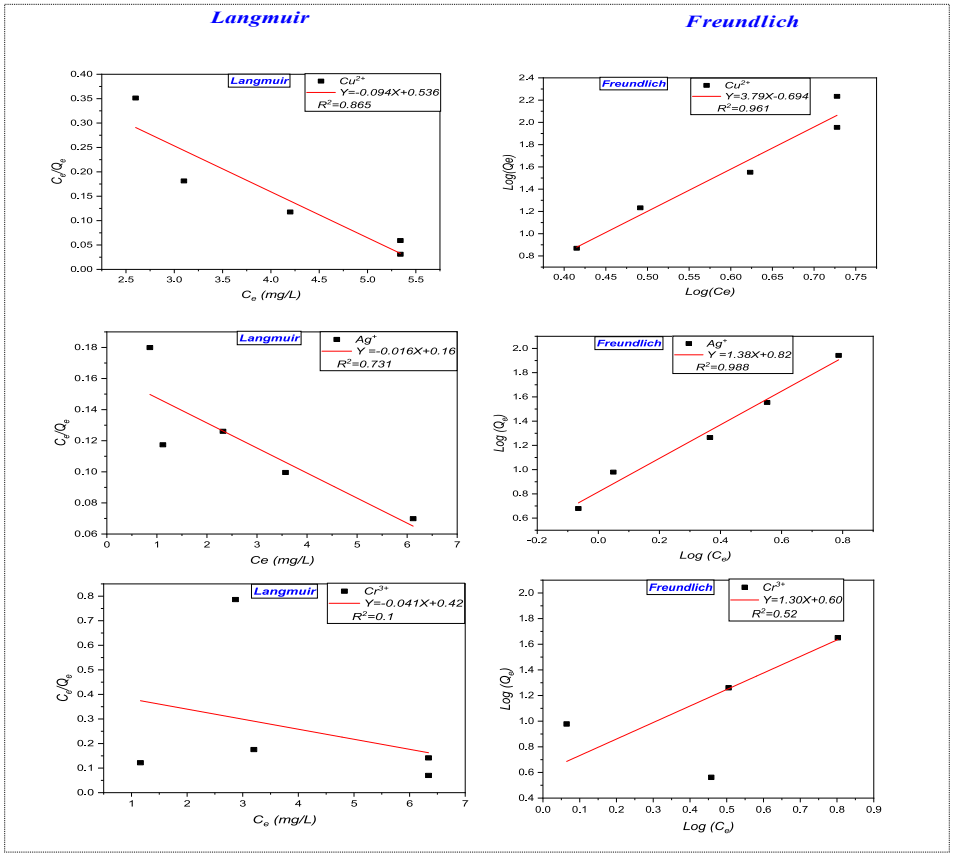

Fig. 11. The Langmuir and Freundlich isothermal models of the adsorption process of Cr (III), Cu (II) and Ag (I) ions on cationic resin A®IRC-50 beads.

Pb^{2+} metal on hausmannite.

magnetic nanoparticles [25,26].

3.2. Effect of the mass

The influence of the different masses of the cationic adsorbent polymer resin on the adsorption process was studied and the results are presented herein. Noteworthy, a range of masses, spanning from 0.05 g to 2 g, was selected for investigation. Each mass was immersed in individual metal solutions containing Cr (III), Cu (II), and Ag (I) at concentrations of 10 ppm. The systems were vigorously stirred at a controlled temperature of 25 °C for a duration of 5 h.

As depicted in Fig. 6, the results obtained revealed an inverse relationship between contact time and the mass of the resin. Notably, an increase in the mass of the resin was concomitant with a decrease in the contact time required for effective adsorption. Concurrently, the adsorption efficiency for the various multivalent metals, including Cr (III), Cu (II), and Ag (I), increases in tandem with the resin mass, ranging from 0.05 to 2.0 g. The adsorption curves illustrate that the removal percentage of inorganic pollutants for these three metals reaches 100% when a mass of 2.0 g of cationic resin is utilized. Consequently, the findings of this study reveal that an increase in the mass of resin utilized results in an increase in the number of coordination sites available for the three multivalent metals, hence, promoting the effective depollution of the water solution being studied [27]. It is worth noting that the adsorption efficiency of 100% was achieved using a resin mass of 0.1 g, which was identified as the optimal mass based on economic considerations.

3.3. Impact of the concentration study

The adsorption behavior of the metallic pollutants, including Cr (III), Cu (II), and Ag (I), on the organic adsorbent was investigated at different concentrations ranging from 10 to 200 mg/L for each metal and the results are depicted in Fig. 7. As evident in Fig. 7, the amount of metals adsorbed reaches saturation rapidly for all concentrations, within approximately 20 min. The adsorption capacity of the cationic resin exhibits a significant increase at the initial stage for higher metal concentrations. However, at a concentration of 100 mg/L for all three metals, a plateau is reached, indicating the maximum saturation of the adsorbent. The corresponding values for this plateau are as follows: $Q_{max} = 90.16$ mg.g^{-1}and 96.60% for Cr (III), $Q_{max} = 87.55$ mg.g^{-1} and 96.62% for Ag (I), and $Q_{max} = 171.33$ mg.g^{-1}and 96.98% for Cu (II). This plateau phenomenon can be attributed to the depletion of active sites available on the surface morphology of the cationic resin [28–30]. These findings are consistent with previous studies on the adsorption behavior of metals and highlight the adsorption capacity and efficiency of the cationic resin in removing metallic pollutants from the solution.

Table 4
Parameters of the pseudo 1st and 2^{sec} order's kinetic models of the different cationic multivalent metals Cr (III), Cu (II) and Ag (I) ions on the cationic polymer organic A®IRC-50 resin beads.

Kinetic	Metal	[C] mg/L	$q_{e\text{-}exp}$ (mg/g)	$q_{e\text{-}calcul}$ (m/g)	k_1 (min^{-1})	R^2
Pseudo 1st order	Cr(III)	10	3.65	3.89	0.026	0.980
		20	9.51	7.94	0.024	0.956
		40	18.23	13.96	0.026	0.916
		100	44.76	38.9	0.024	0.986
		200	90.16	63.09	0.030	0.966
	Cu(II)	10	7.4	7.76	0.0064	0.784
		20	17.09	15.32	0.014	0.828
		40	35.67	26.9	0.017	0.822
		100	90.26	74.13	0.021	0.935
		200	171.33	104.7	0.022	0.860
		10	4.78	3.39	0.028	0.874
		20	9.54	7.76	0.026	0.978
	Ag(I)	40	18.40	16.6	0.024	0.994
		100	35.84	25.7	0.018	0.898
		200	87.55	66.07	0.018	0.942
pseudo 2^{sec} order		20	3.65	6.25	0.0025	0.531
		40	9.51	10.31	0.0049	0.988
	Cr(III)	60	18.23	19.23	0.0043	0.998
		100	44.76	50	0.00097	0.986
		200	90.16	100	0.0012	0.999
		20	7.4	7.69	0.006	0.992
		40	17.09	18.18	0.0038	0.994
	Cu(II)	60	35.67	37.03	0.0034	0.999
		100	90.26	100	0.0007	0.995
		200	171.33	166.67	0.0009	0.999
		20	4.78	5.07	0.014	0.993
		40	9.54	10	0.0071	0.995
	Ag(I)	60	18.40	19.6	0.0031	0.996
		100	35.84	38.46	0.0016	0.998
		200	87.55	100	0.0006	0.998

Table 5
Model Parameters.

Langmuir	Metal	Q_{mexp} mg.g^{-1}	Q_{mcal} mg.g^{-1}	K_L ($L.mg^{-1}$)	R^2
	Cr (III)	90.16	−24.39	−0.097	0.52
	Cu(II)	171.33	−10.63	−0.17	0.961
	Ag(I)	87.55	−62.5	−0.1	0.955
Temkin	**Metal**	**B_1**	**ΔQ (kJ.mol^{-1})**	**K_T**	**R^2**
	Cr (III)	37.71	93.43	1.39	0.55
	Cu(II)	0.004	9.91	1.00	0.81
	Ag(I)	0.002	54.51	78.25	0.82
Freundlich	**Metal**	**1/n**	**N**	**K_F**	**R^2**
	Cr (III)	1.30	0.75	3.98	0.52
	Cu(II)	3.79	0.26	0.20	0.961
	Ag(I)	1.36	0.73	3.31	0.955

The cationic adsorbent resin organic exhibits a saturation capacity of 90.16 mg/g for Cr (III), 171.33 mg/g for Cu (II), and 87.55 mg/g for Ag (I) when loaded with the metal ions. This behavior can be explained by the concentration-dependent interactions between the adsorbent and the metal ions in the solution. At low concentrations, the ratio of active sites on the cationic resin to the total metal ions in the solution is high. Consequently, all the inorganic ions can be effectively retained and completely separated from the solution by the adsorbent. However, at higher concentrations, the driving force for adsorption, caused by the concentration gradient, becomes stronger. As a result, greater quantities of different metal ions, such as Cr (III), Cu (II), and Ag (I), are adsorbed per unit mass of the adsorbent (qe), leading to resin saturation. This saturation point results in a lower adsorption yield, as some ions remain unbound in the solution [31–34]. Therefore, it can be concluded that the cationic resin adsorbent is particularly effective for treating wastewater with low concentrations of various metal ions, where the adsorption process is more favorable and efficient.

3.4. Effect of temperature

To investigate the impact of temperature on the adsorption intensity of metal solutions on the cationic resin A®IRC-50, experiments were conducted using 0.1 g of the resin with a 100.0 mL solution containing different metal ions (Cr (III), Cu (II), and Ag (I)). Noteworthy, the adsorption studies were performed at various temperatures ranging from 298 K to 328 K, as depicted in Fig. 8. The adsorption capacity of the resin for the three metal solutions exhibited a slight increase with temperature, suggesting that the adsorption process of the metal ions from the metallic solution is likely to be an endothermic phenomenon [35,36]. The higher temperature facilitates stronger interactions between the resin and the metal ions, resulting in enhanced adsorption capacity.

As depicted in Fig. 8, the efficiency of the removal of the different metals showed a slight increase (almost constant) as the temperature was raised from 25 °C to 55 °C. Specifically, the percentage of removal for Cr (III) increased from 60% to 84.15%, for Ag (I), it increased from 84.65% to 93.15%, and for Cu (II) it increased from 55% to 96.2%.

The observed increase in adsorption efficiency with temperature suggests that the adsorption process can be classified as endothermic. This can be attributed to the fact that higher temperatures facilitate the agglomeration of multivalent metal cations on the surface of the cationic resin beads.

3.5. Kinetic adsorption models

The adsorption kinetics of the different metals, Cr (III), Cu (II), and Ag (I) ions on the cationic resin A®IRC-50, were analyzed using the pseudo-first order and pseudo-second order models to determine the adsorption mechanism and the results are depicted in Figs. 9, 10, 11 and Table 4.

As evident in Fig. 10, the pseudo-2^{sec}-order kinetic model present is intelligible in linear form as seen in Eq. (5).

3.6. Adsorption phenomenally isotherm

In the present study, three isotherm models, namely Langmuir, Freundlich, and Temkin, were employed to investigate the distribution of inorganic ions between the aqueous metallic solution and the cationic adsorbent resin A®IRC-50 at equilibrium. These isotherm models provide valuable insights into the adsorption behavior and help in optimizing the quantity of resin utilized [36–40].

3.6.1. Langmuir isothermal process

The Langmuir isotherm model assumes that adsorption occurs on specific and homogeneous sites on the surface of the cationic adsorbent resin A®IRC-50 (Fig.11) [39,40]. The experimental data obtained from the adsorption tests of the different metal ions Cr (III), Cu (II), and Ag (I) on the organic resin were analyzed using the Langmuir model by the equation found in Table 5.

3.6.2. Freundlich adsorption isotherm

The Freundlich isotherm model assumes a multilayer adsorption phynomenally process and considers the solid surface morphology of the adsorbent organic resin to be heterogeneous [41,42]. The Freundlich equation, in its linear form, is given by the equation shown in Table 5.

According to the results presented in Table 5, the Freundlich isothermal model exhibited a strong correlation with the experimental data as evidenced by the high coefficient of determination (R^2). The calculated single-layer adsorption capacities closely approximated the experimental values of the maximum adsorption capacity, with only

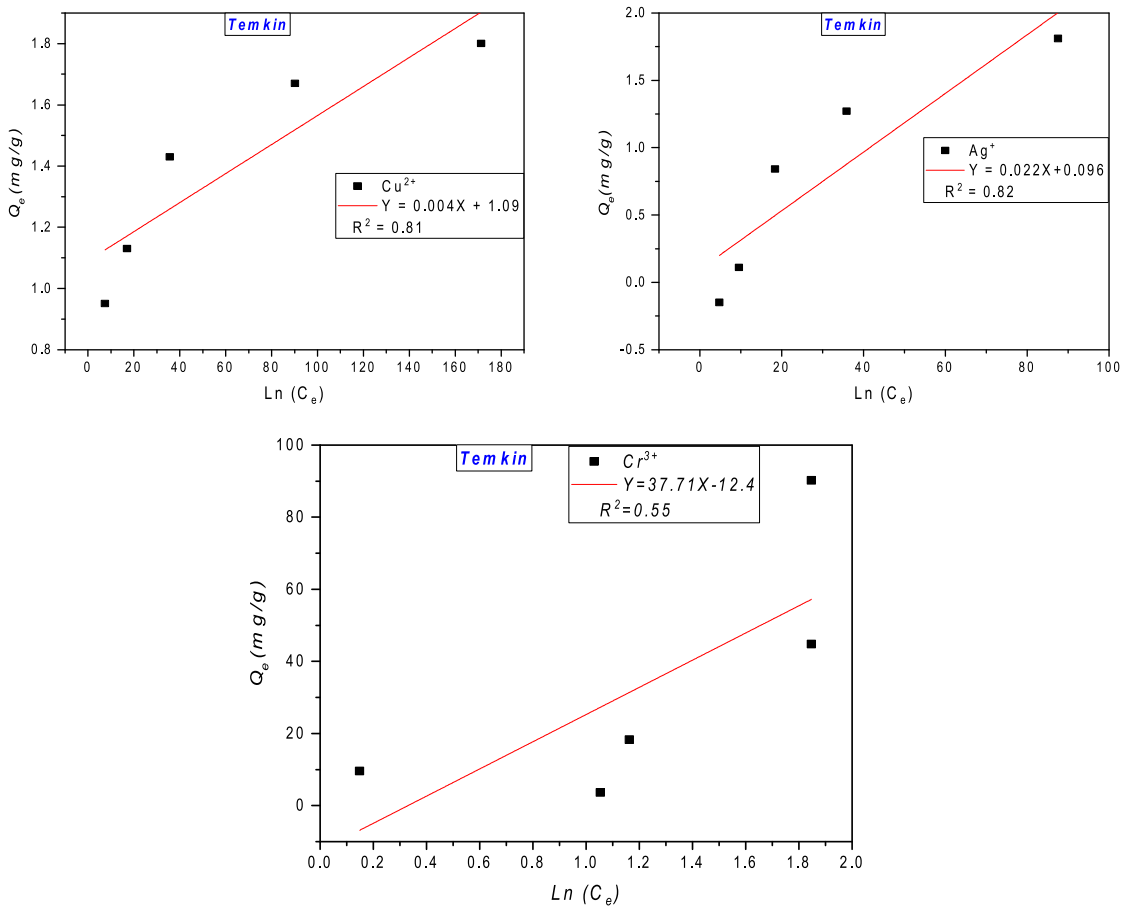

Fig. 12. Temkin of Cr (III), Ag (I) and Cu (II) adsorption on the A®IRC-50 resin.

minor deviations observed for the heavy multivalent metal ions.

3.6.3. *Temkin present adsorption phenomenally isothermal*

The Temkin isothermal equation provides insight into the heat of adsorption in the adsorption process of the metal ions being studied, from the metallic solution onto the cationic resin A®IRC-50 beads. The results revealed that the heat of adsorption decreases linearly with coverage due to the interactions between the adsorbent and the metal ions, indicating an ordered allocation of binding energies. This energy allocation persists until a certain energy threshold is reached (93.43 Kj. mol^{-1}) [43]. The linear form of the Temkin isothermal model is expressed by the equation provided in Table 5. In this equation, qe represents the adsorbent's capacity at equilibrium ($mg.g^{-1}$), the concentration of the cationic resin at equilibrium ($mg.L^{-1}$), $RT/\Delta Q = B1$, where T is the temperature in Kelvin (K), R is the ideal gas constant (8.314 $J.mol^{-1}$. K^{-1}), and ΔQ represents the difference in adsorption energy of the aqueous solution.A linear plot of Qe vs Ce as depicted in Fig. 12 allowed the determination of the different parameters present. The constant ΔQ present is related to the heat of the process adsorption process. Based on the different values of A and B_1 obtained from the analysis and presented in Table 5, the adsorption process of the various metals Cr (III), Cu(II) and Ag(I) on A®IRC-50 cationic resins can be deduced to be primarily driven by physisorption, as evident by the value of (ΔQ) which is greater than 40 $kJ.mol^{-1}$ [44].

3.7. *Thermodynamic party of adsorption phenomenally*

The parameters thermodynamic, including the change in (ΔG°) [Gibbs free energy], the (ΔH°)[enthalpy change], and (ΔS°)[the entropy change], play a crucial role in understanding the effect of temperature on the adsorption of multivalent metal ions on the cationic adsorbent resin A®IRC-50 and provide information detailed on the various inherent energies associated with the process (Fig.13) [45]. The values of ΔH° and ΔS° can be determined using the relationships provided in Table 6.

The positive values of the enthalpy change (ΔH°) indicate that the adsorption process of the various metal ions on the cationic polymeric organic resin A®IRC-50 is endothermic [46].

This suggests that the adsorption process requires the input of heat energy. Furthermore, the magnitude of the positive ΔH° values, suggests that the adsorption process is of the physisorption type [47]. Noteworthy, the positive values of ΔG° indicate that the adsorption process is spontaneous and thermodynamically favorable.

The positive values of ΔS° suggest an increase in disorderliness or randomness at the interface between the cationic polymer resin and the cationic multivalent metal solution.

3.8. *Regeneration of the resin*

To test the reversibility of A®IRC-50 cationic resin, the support recovered from the extraction kinetics study was brought into contact with 100 mL of 0.1 M HCl and 0.1 M H_2SO_4 solution. Fig. 14 shows the desorption kinetics of the metals retained for an initial concentration of 10 ppm for (Ag(I) and Cr(III)) and Cu(II) by the cationic resin A®IRC-50.

Fig. 14 shows that desorption is more and similar to those found in the case of bivalent metals is slow for the trivalent metal (Chromium). Equilibrium is reached after 30 min for the cationic resin A®IRC-50 in the medium of HCl, whereas in the medium of H_2SO4 equilibrium is reached after 50 min, with a desorption rate of 99.8% for both media [49].

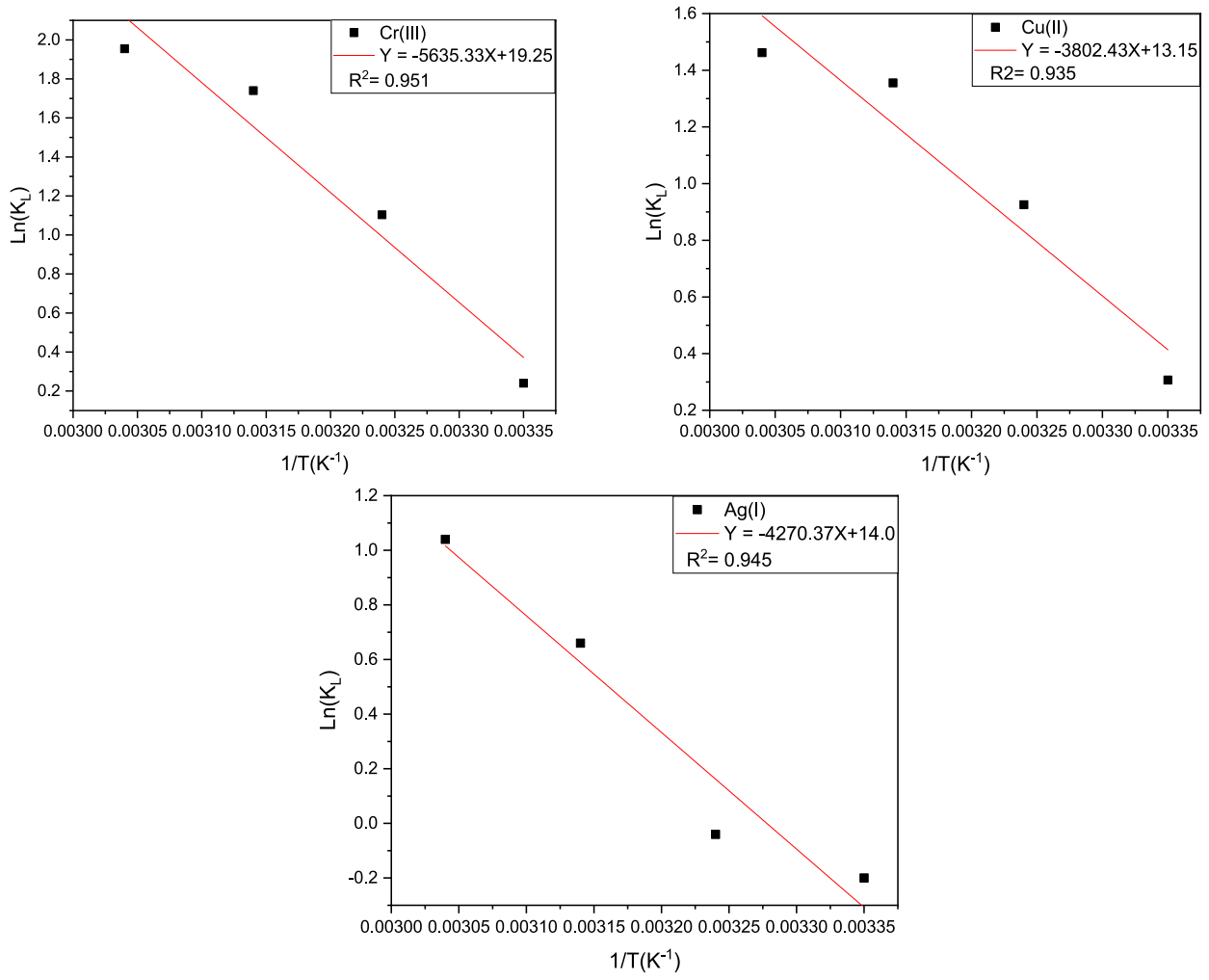

Fig. 13. The Van 't Hoff of the various metals Cr(III), Cu(II) and Ag(I) adsorption curve on the cationic resin A®IRC-50.

Table 6
Thermodynamic Parameters:

Metal	T (K)	1/T (K^{-1})	ΔG° ($kJ.mol^{-1}$)	ΔH° ($kJ.mol^{-1}$)	ΔS° ($J.mol^{-1}.K^{-1}$)
	298	0.00335	−0.83		
Cr(III)	308	0.00324	−2.44		
	318	0.00314	−4.04	46.85	160.04
	328	0.00304	−5.64		
	298	0.00335	−0.873		
Cu(II)	308	0.00324	−2.06		
	318	0.00314	−3.15	31.61	109.33
	328	0.00304	−4.25		
	298	0.00335	0.81		
Ag(I)	308	0.00324	−0.35		
	318	0.00314	−1.51	35.50	116.40
	328	0.00304	−2.68		

3.9. Mechanism of adsorption of the different multivalent metals Ag(I), Cu(II) and Cr(III) ions

The adsorption mechanisms involved in the binding of various cationic multivalent metal ions are complex and depend on factors such as the specific cationic polymer resin used and the nature of the metal ions present. Among the various mechanisms proposed, ion exchange was considered to be the most significant process in the cationic resin adsorption being studied herein [23]. The exchange of various multivalent metal ions on the cationic polymeric resin can be reversible, allowing for the recovery of the adsorbed metal ions through the acid wash with HCl [24,43]. The specific complexation mechanism of the cationic multivalent metal ions on the adsorbent cationic polymeric resin can be visualized and understood through the analysis of Fig. 16.

Cationic polymeric resins typically have porous walls composed of a solid amorphous matrix, which is primarily composed of organic polymers [26,48]. These resins contain various functional groups that can contribute to the adsorption of multivalent metal ions, including Cr(III), Cu(II), and Ag(I), as well as participate in complexation reactions. The presence of oxygen and phosphonate groups has been identified in the morphology of the organic polymer under investigation [27]. It is important to note that the existence of a particular functional group does not necessarily indicate a single adsorption mechanism, as the same functional group can participate in multiple mechanisms.

In addition to ion exchange, the oxygen atoms in the resin have been observed to form complexes with Ni (II) through complexation reactions [28,29]. Similarly, phosphate groups have been found to form complexes with Cr (III), Cu (II), and Ag (I) metal ions [2]. It is crucial to recognize that determining the adsorption mechanism solely based on the presence of functional groups in the cationic resin may not provide an accurate understanding. However, previous research has demonstrated that the oxygen groups on the cationic resin are primarily responsible for the adsorption of Cr (III), Cu (II), and Ag (I) metal ions through the ion exchange mechanism [31].

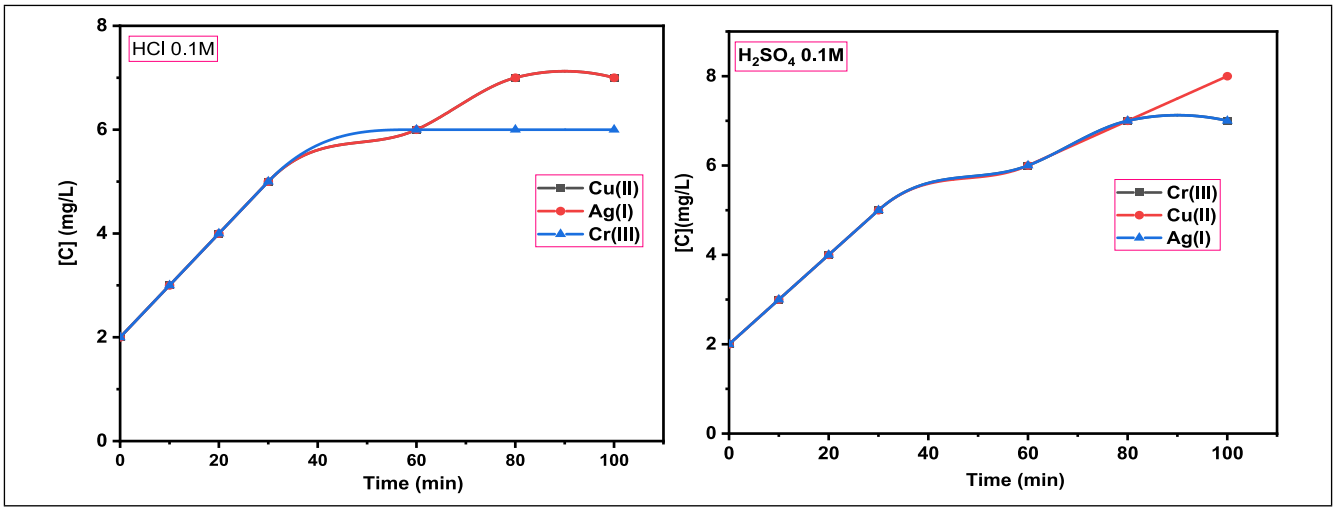

Fig. 14. Study of the kinetics of desorption of various metals by the cationic resin Amberlite®IRC-50.

3.10. Molecular dynamics simulation

Monte Carlo simulations have indeed been widely used to study and predict the interactions between adsorbate molecules and metal surfaces, including the multivalent metal ions Cr(III), Cu(II), and Ag(I). The results of the simulation conducted in this study are presented herein.

The energy change exhibits a gradual decrease as the number of optimization steps increases. Initially, the energy tends to minimize due to the inherent instability of the $C_{23}H_{37}Cl_2N_3O$. Subsequently, with continued optimization, the total energy reaches a state of stability, as depicted in Fig. 15.

Furthermore, Fig. 16 depicts the relationship between the convergence of the optimization geometry and the number of optimization steps. Noteworthy, the Conjugate Gradient optimization method was utilized to process the $C_{23}H_{37}Cl_2N_3O$. The figure reveals a gradual decrease in both the energy change and the gradient value as the number of optimization steps increases. This phenomenon arises from the progressive completion of crystallization growth in the $C_{23}H_{37}Cl_2N_3O$, occurring within a low-temperature crystallization state [48].

The energy distributions of the organic resin molecules on the different metals being studied are depicted in Figs. 17, 18, and 19. These figures depict various energy components, including total energy, average total energy, van der Waals energy, electrostatic energy, and intermolecular energy. Notably, van der Waals energy emerged as the dominant form of interaction energy for both adsorbents.Fig. 20.

Furthermore, Figs. 17, 18, and 19 also depict the most stable and low-energy adsorption configurations (at a 1:1 ratio) of the resin polymeric molecules on different metal surfaces. These configurations were determined through Monte Carlo simulation, with the energy optimization process. Table 7 provides the outputs and descriptors, including total adsorption energy, rigid adsorption process, and deformation energies. The adsorption energy study investigates the energy released during the relaxed adsorbate on the metallic solution, encompassing various components of adsorption (Fig. 20).

The adsorption process energy is calculated as the sum of the adsorption solid energy and the energy deformation of the adsorbate component. More negative adsorption energy values indicate a stronger and more favorable interaction between the metal surface and the inhibitor molecule. Based on the results presented in Table 7, it is evident that the negative adsorption energies of the resin polymeric molecules on different metal surfaces follow the order of Cu(II) > Ag (I) > Cr (III).

4. Comparative studies on the adsorption of the various metals ions by the resin

Some authors have focused on increasing the resin, thus demonstrating a proportional relationship between their number and the quantity of ions fixed, Table 8 gives some examples of the various adsorbents of natural polymers for use as adsorbents.

The chemical resin and the adsorbent that resulted were the subject of a review. The majority of the halogenation, etherification, and oxidation techniques were explored and used to the adsorbent. The adsorption outcomes are quantitatively dependent on the chemical alteration used as well as the metals used. They're also tough to compare due to the wide range of experimental circumstances used by the many authors. In the case of Cr(III), Cu(II) and Ag(I), the best retention capabilities are obtained.

5. Conclusion

Summarily, the adsorption process of various multivalent metal ions utilizing a cationic organic polymer resin A®IRC-50 was studied in a metallic solution using different metals including Cr (III), Cu (II) and Ag (I). The impact of the contact time, temperature, and isothermal models on the efficacy of the adsorption process was assessed while the adsorption mechanism was also determined. In molecular dynamic simulation calculations, it has an adsorption energy value of −119.42 kcal.mol^{-1} between the studied molecule and Cr(III) metal, −94.24 kcal.mol^{-1} adsorption energy between Ag(I) metal, and −93.57 kcal.mol^{-1} between Cu(II) metal. It has been observed that it has an energy value of /mol. it was observed that this interaction was more stable with the adsorption energy value of −119.42 kcal.mol^{-1}. Conclusively, the results of this analysis found A®IRC-50 worthy of being used as an adsorbent in adsorption processes due to its efficacy as evident in the results of this study and the economic advantage it offers in the treatment of wastewater containing multivalent heavy metals.

CRediT authorship contribution statement

Jaouad Bensalah: Conceptualization, Data curation, Formal analysis, Investigation, Methodology, Writing – original draft, Writing – review & editing. **Hanae Ouaddari:** Data curation, Formal analysis, Methodology, Writing – review & editing. **Şaban Erdoğan:** Data curation, Formal analysis, Methodology, Writing – review & editing. **Burak Tüzün:** Data curation, Formal analysis, Methodology, Writing – review & editing. **Abdel-Rhman Z Gaafar:** Data curation, Formal analysis,

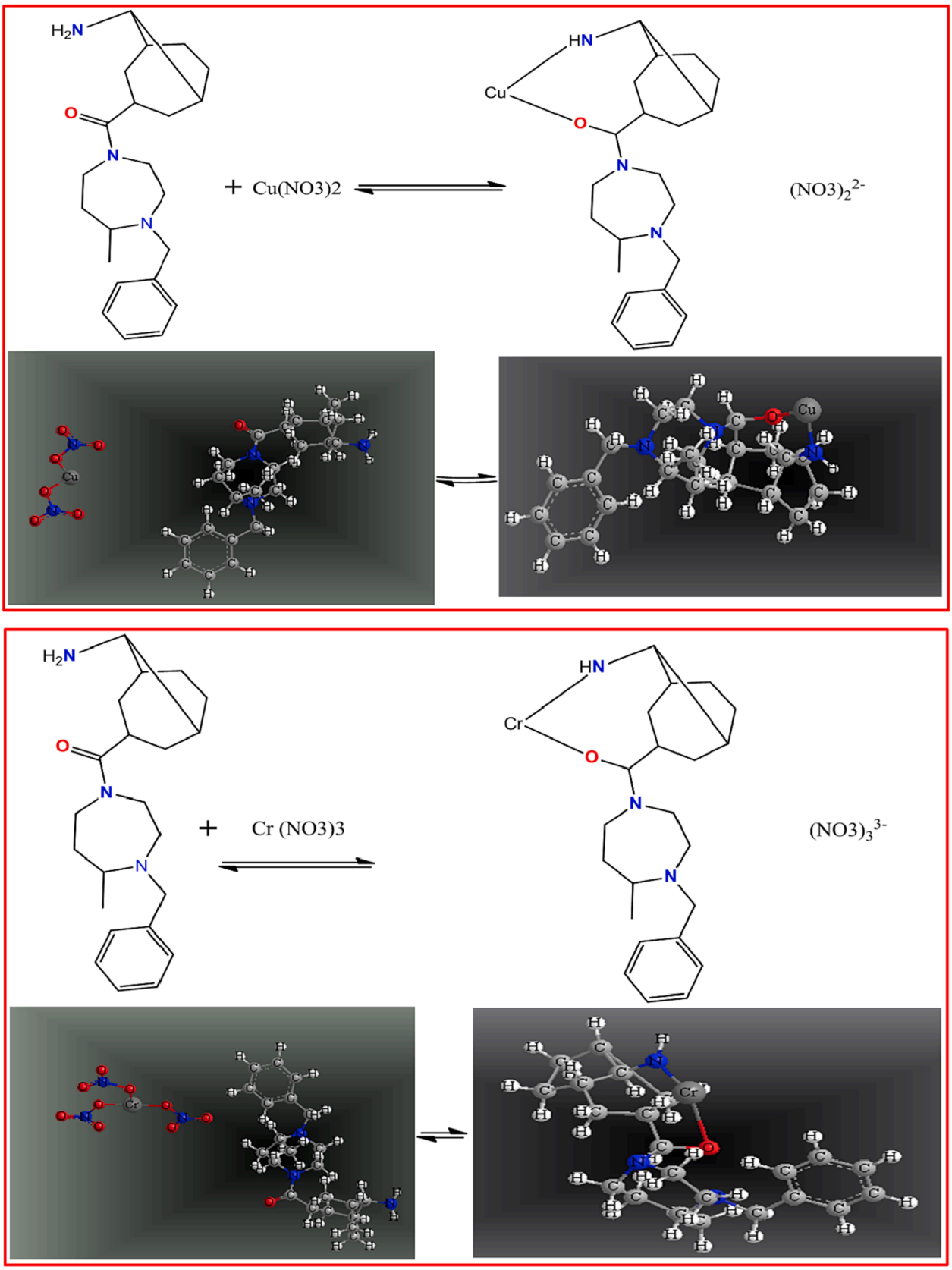

Fig. 15. Possible mechanisms of the binding of the different multivalent ions to the cationic polymer organic adsorbent.

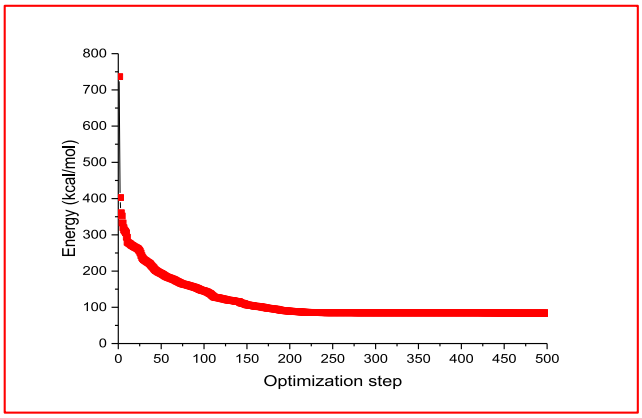

Fig. 16. Forcite geometry optimization energy plot of the molecule adsorbent organic.

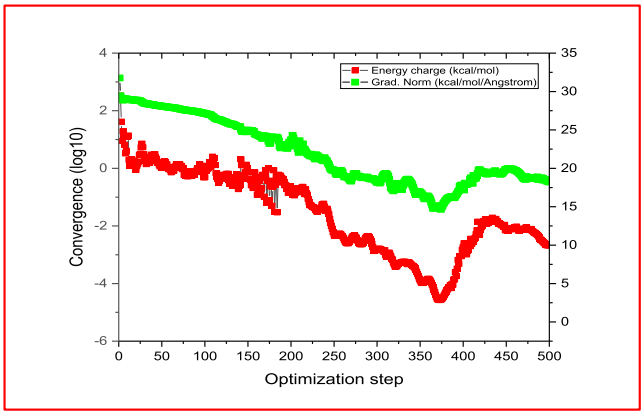

Fig. 17. Forcite geometry optimization- convergence plot molecule organic resin present.

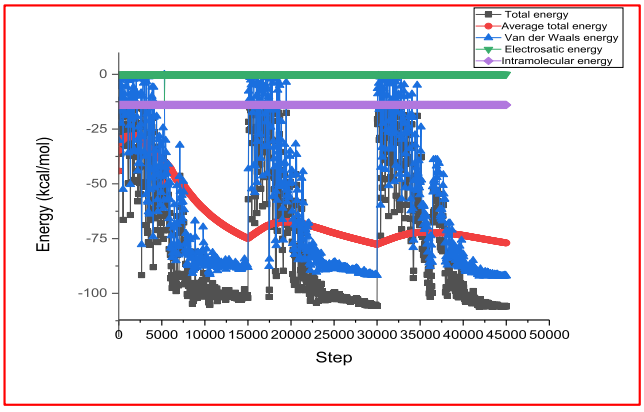

Fig. 18. Total energy value between molecule organic resin and the metal Cr(III).

Methodology, Writing – review & editing. **Hiba-Allah Nafidi:** Writing – review & editing, Data curation, Formal analysis, Methodology. **Mohammed Bourhia:** Writing – review & editing. **Amar Habsaoui:** Conceptualization, Formal analysis, Investigation, Methodology, Project administration, Resources, Supervision, Software, Writing – original draft, Writing – review & editing.

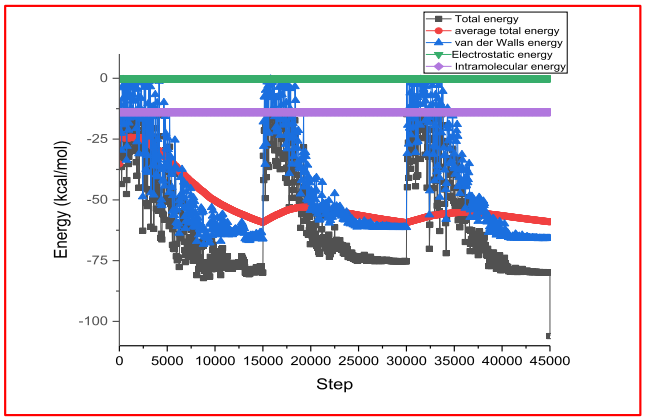

Fig. 19. Total energy value between molecule adsorbent organic resin and the metal Ag(I).

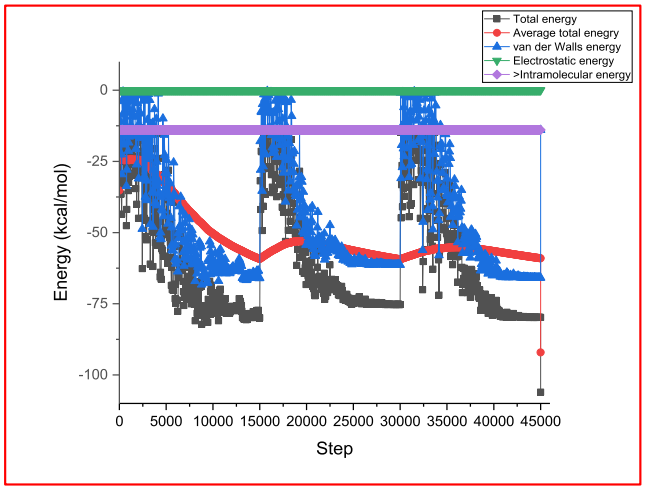

Fig. 20. Total energy value between molecule resin polymeric and the metal Cu(II).

Table 7
Experimental adsorption efficiencies, the outputs and calculated descriptors by the simulation (Mont Carlo) for the adsorption of the resin polymeric on the various metals present.

Metal	Total energy	Adsorption energy	Rigid adsorption energy	Deformation energy
Cr (III)	−133.37	−119.42	−110.00	−9.41
Ag (I)	−108.19	−94.24	−81.97	−12.27
Cu (II)	−107.52	−93.57	−85.52	−8.05

Table 8
Examples of some the resin for use as the metals ion adsorbents.

Adsorbent	Rendement en %	Reference
Cellulose	80.00	[49,50]
Remove of the MO dye	80.20	[51]
Remove of the Co (II)	90.00	[52]
Remove of the multivalent metals (Cr(III), Cu(II) and Ag(I))	*71% for Cr (III), 74% for Cu (II), 91.78% for Ag (I).*	*This Works*

Declaration of Competing Interest

The authors declare that they have no known competing financial interests or personal relationships that could have appeared to influence the work reported in this paper.

Data availability

No data was used for the research described in the article.

Acknowledgments

University Center for Analysis, Technology and Incubation Transfer Expertise (CUAE2TI), under the Ibn Tofaïl University of Kenitra, and the National Center for Scientific and Technical Research CNRST of Morocco have made available to the scientific equipment of the UATRS division.

The authors extend their appreciation to the Researchers Supporting Project number (RSPD2023R686) King Saud University, Riyadh, Saud Arabia.

"I, **Jaouad Bensalah** (the Corresponding Author), on behalf of other authors declare that this manuscript is original, has not been published before and is not currently being considered for publication elsewhere. There is also no conflict of interest in any way. There is not any competing interested too.

References

[1] B. Abbou, I. Lebkiri, H. Ouaddari, L. Kadiri, A. Ouass, A. Habsaoui, A. Lebkiri, E. H. Rifi, Removal of Cd(II), Cu(II), and Pb(II) by adsorption onto natural clay: a kinetic and thermodynamic study, Turk J Chem. (2021), https://doi.org/10.3906/kim-2004-82.

[2] K. Naseem, Z.H. Farooqi, R. Begum, M.Z. Ur Rehman, M. Ghufran, W. Wu, J. Najeeb, A. Irfan, Synthesis and characterization of poly(N-isopropylmethacrylamide-acrylic acid) smart polymer microgels for adsorptive extraction of copper(II) and cobalt(II) from aqueous medium: kinetic and thermodynamic aspects, Environ. Sci. Pollut. Res. 27 (22) (2020) 28169–28182.

[3] A. Nobakht, D. Jafari, M. Esfandyari, New insights on the adsorption of phenol red dyes from synthetic wastewater using activated carbon/Fe2(MoO4)3, Environ. Monit. Assess. 195 (5) (2023).

[4] K. Kiani Zadeh, D. Jafari, Activated carbon/alginate/Fe3O4 magnetic nanocomposite as a superior functional material for removal of lead from aqueous media, Biomass Convers. Biorefin. 99(2023).

[5] M. Zahed, D. Jafari, M. Esfandyari, Adsorption of formaldehyde from aqueous solution using activated carbon prepared from Hibiscus rosa-sinensis, Int J Environ Anal Chem. 102 (2020) 2979–3001, https://doi.org/10.1080/03067319.2020.1762872.

[6] E. Aboli, D. Jafari, H. Esmaeili, Heavy metal ions (lead, cobalt, and nickel) biosorption from aqueous solution onto activated carbon prepared from Citrus limetta leaves, Carbon Lett. 30 (6) (2020) 683–698.

[7] K. Naseem, R. Huma, A. Shahbaz, J. Jamal, M.Z. Ur Rehman, A. Sharif, E. Ahmed, R. Begum, A. Irfan, A.G. Al-Sehemi, Z.H. Farooqi, Extraction of Heavy Metals from Aqueous Medium by Husk Biomass: Adsorption Isotherm, Kinetic and Thermodynamic study, Z. Phys. Chem. (2018), https://doi.org/10.1515/zpch-2018-1182.

[8] K. Naseem, Z.H. Farooqi, R. Begum, M.Z. Ur Rehman, A. Shahbaz, U. Farooq, M. Ali, H.M.A. Ur Rahman, A. Irfan, A.G. Al-Sehemi, Removal of Cadmium (II) from Aqueous Medium Using Vigna radiata Leave Biomass: Equilibrium Isotherms, Kinetics and Thermodynamics, Z. Phys. Chem. 233 (5) (2019) 669–690, https://doi.org/10.1515/zpch-2018-1223.

[9] K. Naseem, R. Begum, W. Wu, M. Usman, A. Irfan, A.G. Al-Sehemi, Z.H. Farooqi, Adsorptive removal of heavy metal ions using polystyrene-poly (N-isopropylmethacrylamide-acrylic acid) core/shell gel particles: Adsorption isotherms and kinetic study, J. Mol. Liq. 277 (2019) 522–531, https://doi.org/10.1016/j.molliq.2018.12.054.

[10] J. Bensalah, M. Berradi, A. Habsaoui, M. Allaoui, H. Essebaai, O. El Khattabi, A. Lebkiri, E.H. Rifi, Kinetic and thermodynamic study of the adsorption of cationic dyes by the cationic artificial resin Amberlite®IRC50, Mater Today. (2021), https://doi.org/10.1016/j.matpr.2021.02.028.

[11] J. Bensalah, A. Habsaoui, B. Abbou, L. Kadiri, I. Lebkiri, A. Lebkiri, E.H. Rifi, Adsorption of the anionic dye methyl orange on used artificial zeolites: kinetic study and modeling of experimental data, Mediterr J Chem. 9 (4) (2019) 311–316.

[12] I.D. Mall, V.C. Srivastava, N.K. Agarwal, Removal of Orange-G and Methyl Violet dyes by adsorption onto bagasse fly ashdkinetic study and equilibrium isotherm analyses, Dyes Pigm. 69 (2006) 210–223, 10.1016/j.dyepig.2005.03.013.

[13] D. Kavitha, C. Namasivayam, Experimental and kinetic studies on methylene blue adsorption by coir pith carbon, Bioresour. Technol. 98 (2007) 14–21, 10.1016/j.biortech.2005.12.008.

[14] M. Sinan Bilgili, Adsorption of 4-chlorophenol from aqueous solutions by xad-4 resin: Isotherm, kinetic, and thermodynamic analysis, J. Hazard. Mater. 137 (2006) 157–164, 10.1016/j.jhazmat.2006.01.005.

[15] M.N. Sahmoune, Evaluation of thermodynamic parameters for adsorption of heavy metals by green adsorbents, Environ Chem Lett. 17 (2019) 697–704, https://doi.org/10.1007/s10311-018-00819-z.

[16] M.R. Awual, M.M. Hasan, Novel conjugate adsorbent for visual detection and removal of toxic lead (II) ions from water, Micropor Mesopor Mat. 196 (2014) 261–269, https://doi.org/10.1016/j.micromeso.2014.05.021.

[17] M.M. Dubinin, The potential theory of adsorption of gasesand vapors for adsorbents with energetically non uniformsurfaces, Chem. Rev. 60 (1960) 235–241, https://doi.org/10.1016/j.micromeso.2014.05.021.

[18] G. Thompson, J. Swain, M. Kay, C.F. Forster, The treatmentof pulp and paper mill effluent: a review, Bioresour. Technol. 77 (3) (2001) 275–286.

[19] Ş. Erdoğan, B. Tüzün, Applications of the Effectiveness of Corrosion Inhibitors with Computational Methods and Molecular Dynamics Simulation, Corrosion: Fundamentals and Protection Mechanisms, 2022.

[20] S. N. Das, S. G. Barman, and S. G. Ahuja, Zeolite synthesis and its application as adsorbent. (2011).

[21] V.K. Gupta, I. Ali, T.A. Saleh, M.N. Siddiqui, S. Agarwal, Chromium removal from water by activated carbon developed from waste rubber tires, Environ. Sci. Pollut. Res. 20 (3) (2013) 1261–1268.

[22] J. Bensalah, A. Habsaoui, O. Dagdag, A. Lebkiri, I. Ismi, E.H. Rifi, I. Warad, A. Zarrouk, Adsorption of a cationic dye (Safranin) by artificial cationic resins Amberlite®IRC-50: Equilibrium, kinetic and thermodynamic study, Chem. Data Coll. 35 (2021), 100756. / 10.1016/j.cdc.2021.100756.

[23] A.E. Burakov, E.V. Galunin, I.V. Burakova, A.E. Kucherova, S. Agarwal, A. G. Tkachev, V.K. Gupta, Adsorption of heavy metals on conventional and nanostructured materials for wastewater treatment purposes: A review, Ecotoxicol. Environ. Saf. 148 (2018) 702–712.

[24] M.P. Pico, A. Romero, S. Rodríguez, A. Santos, Etherification of glycerol by tert-butyl alcohol: kinetic model, Ind. Eng. Chem. Res. 51 (28) (2012) 9500–9509.

[25] J.H. Chen, W.-R. Chen, Y.-Y. Gau, C.-H. Lin, The preparation of di (2-ethylhexyl) phosphoric acid modified Amberlite 200 and its application in the separation of metal ions from sulfuric acid solution, React Funct Polym. 56 (2003) 175–188, https://doi.org/10.1016/S1381-5148(03)00056-7.

[26] S. Rangabhashiyam, S. Lata, P. Balasubramanian, Biosorption characteristics of methylene blue and malachite green from simulated wastewater onto Carica papaya wood biosorbent. Surf, Interfaces 10 (2018) 197–215. / 10.1016/j.surfin.2017.09.011.

[27] E.-H. Rifi, D. Lakkis, J.M. Leroy, Extraction de l'argent par des gels d'acide polyacrylique–polyacrylate de sodium. Application à l'élimination des ions chlorures, C. R. Chim. 8 (2005) 917–921, 10.1016/j.crci.2004.12.011.

[28] J. Li, Z. Wang, J. Wang, J. Gao, M. Zou, Y. Li, et al., Spectroscopic investigation on the sonodynamic activity of Safranine T to bovine serum albumin damage, J Lumin. 132 (2012) 282–288, https://doi.org/10.1016/j.jlumin.2011.09.014.

[29] V.K. Gupta, R. Jain, M. Shrivastava, A. Nayak, Equilibrium and thermodynamic studies on the adsorption of the dye tartrazine onto waste "coconut husks" carbon and activated carbon, J. Chem. Eng. Data 55 (2010) 5083–5090.

[30] V.K. Gupta, A. Nayak, S. Agarwal, I. Tyagi, Potential of activated carbon from waste rubber tire for the adsorption of phenolics: Effect of pre-treatment conditions, J. San Eng Division 89 (1963) 31–60, 10.1016/j.jcis.2013.11.067.

[31] M.J. Charrier, E. Guibal, J. Roussy, B. Delanghe, P. Le Cloirec, Vanadium (IV) sorption by chitosan: Kinetics and equilibrium, Water Res. 30 (1996) 465–475.

[32] S. Agarwal, I. Tyagi, V.K. Gupta, M.H. Dehghani, J. Jaafari, D. Balarak, M. Asif, Rapid removal of noxious nickel (II) using novel γ-alumina nanoparticles and multiwalled carbon nanotubes: Kinetic and isotherm studies Turkish, J Eng Env Sci. 32 (2008) 303–312, 10.1016/j.molliq.2016.10.032.

[33] W. Qiu, Y. Zheng, Removal of lead, copper, nickel, cobalt, and zinc from water by a cancrinitetype zeolite synthesized from fly ash, Chem. Eng. J. 145 (2009) 483–488, https://doi.org/10.1016/j.cej.2008.05.001.

[34] H. Kaur, R. Kaur, "Removal of Rhodamine-B dye from aqueous solution onto pigeon dropping: adsorption, kinetic, equilibrium and thermodynamic studies, J Mater Environ Sci. 5 (2013) 1830–1838.

[35] F. Fu, Q. Wang, Removal of heavy metal ions from wastewaters: A review, J Environ Manage. 92 (2011) 407–418, https://doi.org/10.1016/j.jenvman.2010.11.011.

[36] K.R. Hall, L.C. Eagleton, A. Acrivos, T. Vermeulen, Pore-and solid-diffusion kinetics in fixed-bed adsorption under constant-pattern conditions, Ind. Eng. Chem. 5 (1966) 212–223.

[37] P. Shekinah, K. Kadirvelu, P. Kanmani, V Subburam Senthilkumar, Adsorption of lead(II) from aqueoussolution by activated carbon prepared from Eichhornia, J. Chem Technol Biotechnol. 77 (2002) 458–464, https://doi.org/10.1002/JCTB.576.

[38] B. Kiran, A. Kaushik, Chromium binding capacity of Lyngbya putealis exopolysaccharides, Biochem Eng J. 38 (2008) 47–54, https://doi.org/10.1016/j.bej.2007.06.007.

[39] T. Ngulube, J.R. Gumbo, V. Masindi, A. Maity, An update on synthetic dyes adsorption onto clay based minerals: A state-of-art review, J Environ Manage. 191 (2017) 35–57, https://doi.org/10.1016/j.jenvman.2016.12.031.

[40] V.S. Mane, I.D. Mall, V.C. Srivastava, Kinetic and equilibrium isotherm studies for the adsorptive removal of Brilliant Green dye from aqueous solution by rice husk

ash, J Environ Manage. 84 (2007) 390–400, https://doi.org/10.1016/j.jenvman.2006.06.024.
[41] A.R.M. Prates, Hollow Beta zeolites: synthesis and impact of the hollow morphology on diffusion and catalysis, Université de Lyon. (2019), https://doi.org/10.1016/j.micromeso.2020.110499.
[42] M. Gackowski, K. Tarach, Ł. Kuterasiński, J. Podobiński, S. Jarczewski, P. Kuśtrowski, J. Datka, Hierarchical zeolites Y obtained by desilication: Porosity, acidity and catalytic properties, Hierarchical zeolites Y obtained by desilication: Porosity, acidity and catalytic properties. micropor mesopor Mat. 263 (2018) 282–288.
[43] N. Nuttens, D. Verboekend, A. Deneyer, J. Van Aelst, B.F. Sels, Potential of Sustainable Hierarchical Zeolites in the Valorization of α-Pinene, Chem Sus Chem. 8 (2015) 1197–1205, 10.1002/cssc.201403457.
[44] M. Ghaedi, S. Hajjati, Z. Mahmudi, I. Tyagi, S. Agarwal, A. Maity, et al., Modeling of competitive ultrasonic assisted removal of the dyes–Methylene blue and Safranin-O using Fe3O4 nanoparticles, Chem Eng J. 268 (2015) 28–37, https://doi.org/10.1016/j.cej.2014.12.090.
[45] S. Rangabhashiyam, S. Lata, P. Balasubramanian, Biosorption characteristics of methylene blue and malachite green from simulated wastewater onto Carica papaya wood. biosorbent Surf, Interfaces 10 (2018) 197–215, https://doi.org/10.1155/2020/8318049.
[46] B. Benguella, A. Yacouta-Nour, Removal of acid dyes in aqueous solution by bentonite and kaolin, C. R. Chim. 12 (2009) 762–771, https://doi.org/10.1016/j.crci.2008.11.008.
[47] I. Lebkiri, B. Abbou, L. Kadiri, A. Ouass, Y. Essaadaoui, A. Habssaoui, Removal of methylene blue dye from aqueous solution using a superabsorbant hydrogel the polyacrylamide: isotherms and kinetic studies, Mediterr J Chem. 25 (2019) 337–346, https://doi.org/10.13171/mjc941911251089il.
[48] L. Wang, T. Xiao, S. Liu, W. Zhang, B. Yang, L. Chen, Quantification of model uncertainty and variability for landslide displacement prediction based on Monte Carlo simulation, Gondw. Res. (2023).
[49] T. Karmakar, P.M. Piaggi, M. Parrinello, Molecular dynamics simulations of crystal nucleation from solution at constant chemical potential, J. Chem. Theory Comput. 15 (12) (2019) 6923–6930.
[50] S.M. Maliyekkal, K.P. Lisha, T. Pradeep, A novel cellulose–manganese oxide hybrid material by in situ soft chemical synthesis and its application for the removal of Pb (II) from water, J. Hazard. Mater. 181 (1-3) (2010) 986–995.
[51] J. Bensalah, A. Habsaoui, A. Lebkiri, O. El Khattabi, E.H. Rifi, Investigation of the cationic resin Amberlite®IRC-50 as a potential adsorbent to remove the anionic dye methyl orange, Desalin. Water Treat. 246 (2022) 280–290, https://doi.org/10.5004/dwt.2022.27984.
[52] J. Bensalah, A. El Amri, A. Ouass, O. Hammani, L. Kadiri, H. Ouaddari, S. El Mustapha, A. Zarrouk, A. Lebkiri, B. Srhir, E.H. Rifi, Investigation of the cationic resin Am®IRC-50 as a potential adsorbent of Co (II): Equilibrium isotherms and thermodynamic studies, Chem. Data Collect. 39 (2022), 100879, https://doi.org/10.1016/j.cdc.2022.100879.